Desalination and Water Treatment
www.deswater.com
doi: 10.5004/dwt.2017.21506

93 (2017) 163–170
October

Effects of TiO_2 on the laccase enzyme immobilization and the bisphenol-A removal of the ceramic membranes

Samunya Sanguanpak[a,*], Witaya Shongkittikul[a], Anucha Wannagon[a], Chart Chiemchaisri[b]

[a]*National Metal and Materials Technology Center (MTEC), National Science and Technology Development Agency (NSTDA), 114 Thailand Science Park, Pahonyothin Rd., Klong Luang, Pathumthani 12120, Thailand, Tel. +66-256-46500, Fax +66-256-46368, email: samunys@mtec.or.th (S. Sanguanpak), witayas@mtec.or.th (W. Shongkittikul), anuchaw@mtec.or.th (A. Wannagon)*
[b]*Department of Environmental Engineering, Faculty of Engineering, Kasetsart University, Bangkok 10900, Thailand, email: fengccc@ku.ac.th*

Received 10 January 2017; Accepted 1 October 2017

ABSTRACT

This research investigates the effects of titanium dioxide (TiO_2) on the laccase enzyme immobilization and the BPA removal performance of the ceramic membranes. There were four types of experimental ceramic membranes: the ceramic membrane, TiO_2-coated membrane, laccase-immobilized membrane, and laccase-immobilized TiO_2-coated membrane. The laccase concentrations were varied between 0, 500, 2500 and 5000 U L^{-1}. The experimental results revealed that TiO_2 improved the laccase immobilization as TiO_2 increased the membrane surface area, formed the mesoporous structure and induced the stronger binding between the membrane surface and the enzyme. Moreover, the laccase-immobilized TiO_2-coated membrane with 5000 U L^{-1} laccase concentration achieved the highest BPA removal efficiency of 93%. The TiO_2-coated membrane could achieve a higher BPA removal efficiency (31%) than the ceramic membrane (9%) and the 500 U L^{-1} laccase-immobilized membrane (20%). The finding was attributable to the improved degradation of organic pollutants as a result of higher photocatalytic performance under visible light and the enhanced organic-pollutants adsorption capacity of the TiO_2-coated membrane.

Keywords: Ceramic membranes; TiO_2; Laccase enzyme; Bisphenol-A removal

1. Introduction

Micropollutants in water resources, e.g. agricultural pesticides, pharmaceutically active chemicals (PhACs) and endocrine disrupting compounds (EDCs), are harmful to the aquatic ecosystem and human health. In particular, bisphenol A (BPA), an endocrine disrupting compound commonly present in polycarbonates and epoxy resins, is toxic to human health even at low doses [1].

Globally, BPA in wastewater varies from site to site and it greatly depends on the origin of the wastewater, e.g., landfill leachate (200–240 μg L^{-1}) [2], industrial wastewater (0.23–149 μg L^{-1}) [3] and municipal wastewater (0.08–4.98 μg L^{-1}) [3]. Interestingly, small amounts of BPA (0.01–1.08 μg L^{-1}) [3,4] were also reported in the treated municipal wastewater using conventional methods, e.g., the activated sludge (AS). The BPA residues in the treated effluent could be attributed to the fact that most existing conventional wastewater treatment plants were not specifically designed to completely remove BPA [4–6]. Therefore, an improved BPA removal technology to augment the conventional wastewater treatment schemes is necessary.

Meanwhile, the use of biocatalytic enzymes, e.g., laccase, versatile peroxidase and lignin peroxidase, to accelerate the degradation of micropollutants has gained interest in recent years [7]. Specifically, due to its high activity and use of atmospheric oxygen as the final electron acceptor, laccases are a biocatalyst commonly deployed in the wastewater treatment. Furthermore, laccases accelerate the oxidation of phenolic compounds and transform them into large insoluble polymer-reaction products with low toxicity [8]. However, the low reusability and high cost of laccase restrict its independent use in the wastewater treatment, especially on an industrial scale. Therefore,

*Corresponding author.

laccases are immobilized onto solid substrates, including kaolinite, mesoporous silica, chitosan, and membranes. The laccase immobilization also enhances the durability and thermostability under extreme operations [9].

Given the large specific surface area and high enzyme loading capacity, membranes are normally used as the immobilization material for wastewater treatment [10,11]. However, by comparison, ceramic membranes possess greater physical durability, chemical resistance and thermal stability than polymeric membranes [12]. The mechanical strength and morphology of ceramic membranes are subject to the binder type, binder content, fabrication pressure and sintering temperature [13]. According to Chea et al. [10], the gelatin- and laccase-coated ceramic membranes exhibited very high phenolic compounds removal but low permeate flow due to increased membrane fouling.

Hou et al. [14] experimented with the TiO_2-coated, laccase-immobilized hydrophilic polyvinylidene fluoride (PVDF) membranes using the sol-gel coating method; and documented that the TiO_2 coating could substantially enhance the BPA removal and the enzyme stability. However, existing research on TiO_2 and the laccase immobilization centered around the direct immobilization of laccase on the TiO_2 nanoparticles (without the membrane substrate) and the coating of TiO_2 on the commercial polymeric-membrane substrate. On the other hand, this current research focuses on four types of the experimental ceramic membranes: the ceramic membrane, the TiO_2-coated ceramic membrane (TiO_2-membrane), the non-TiO_2-coated ceramic membranes immobilized with laccase (laccase-membrane) and the TiO_2-coated ceramic membranes immobilized with laccase (laccase-TiO_2-membrane). In addition, the physicochemical characteristics and BPA removal performance of the experimental membranes were assessed and compared.

2. Materials and methods

2.1. Materials

This experimental research used the industrial grade calcined alumina powders (SRM30, 99.6 wt% Al_2O_3; Hindalco Industries Ltd.). Carboxymethyl cellulose (CMC) from Sigma-Aldrich was used as the binder in the ceramic membranes. Titanium dioxide (AEROXIDE® TiO_2 P25, Degussa, Germany), Polyethylene Glycol 1000 (PEG1000, Sigma-Aldrich) and ammonium polyacrylate (DispexA40; Ciba, Australia) were used for the preparation of the TiO_2 aqueous suspension. Laccase from *Trametes versicolour* (activity ≥ 0.5 U L^{-1} given 1 mg laccase dissolved in 1 L water) was used, and 3-aminopropyltriethoxysilane (APTES) and glutaraldehyde (GLU) from Sigma-Aldrich were utilized to immobilize the laccase enzyme onto the ceramic membranes. BPA was acquired from Sigma-Aldrich. In addition, 2,2′-Azino-bis (3-ethylbenzothiazoline-6-sulphonic acid) (ABTS, Sigma-Aldrich) was used for the enzymatic activity assay.

2.2. Preparation of the experimental ceramic membranes

The ceramic membranes were fabricated by mixing calcined alumina powders with 1 g L^{-1} CMC solution, where the CMC content in the solution was varied between 0.5, 1.0, 1.5, 2.0 and 2.5 mL per 15 g of calcined alumina powders. The pre-wetted alumina powders were then hydraulically pressed under a 31 MPa uniaxial pressure into disks before sintering at 1,350°C for 1 h under the 3°C min^{-1} heating rate.

The TiO_2-membranes were fabricated by dip-coating the ceramic membranes in 1 g L^{-1} TiO_2 aqueous suspension. The TiO_2 aqueous suspension was prepared by mixing TiO_2 P25 powders with PEG1000 (1:1). Given the TiO_2 nanoparticles aggregation in the aqueous suspension, Dispex A40 of various concentrations (0.0, 0.65, 1.3 and 2.6 wt % relative to the TiO_2 weight) was used to disperse the TiO_2 nanoparticles in the aqueous solution. The aqueous suspension was then coated onto the membrane surface. The TiO_2-coated membranes were then oven-dried at 540°C for 1 h.

Meanwhile, prior to the laccase immobilization, both the ceramic and TiO_2-coated membranes were sequentially modified by 3-Aminopropyltriethoxysilane (APTES) and glutaraldehyde (GLU) according to Hou et al. (2014) [15]. The immobilization of laccase of various concentrations (500, 2500 and 5000 U L^{-1}) was carried out by immerging the ceramic and TiO_2-coated membranes in the laccase solutions at 4°C for 72 h. Fig. 1 illustrates the fabrication process of the four experimental ceramic membranes.

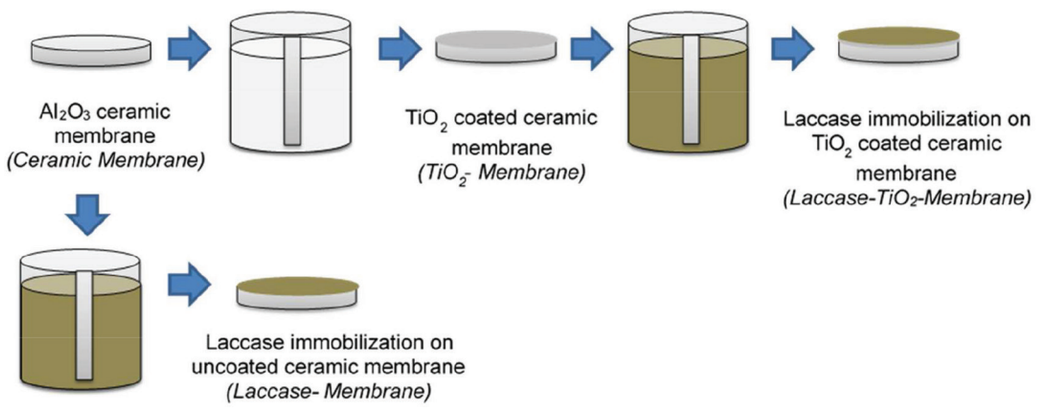

Fig. 1. Schematic of the fabrication process of the four experimental ceramic membranes.

2.3. Characterization of the experimental membranes

The characterization of the four experimental ceramic membranes was then carried out and the results compared. In this research, the proportion of calcined alumina powders to the binder (CMC) was optimized in terms of the bulk density and water absorption of the ceramic membranes in accordance with ASTM C373-88. The tensile strength of the ceramic membranes was determined using the diametral compression testing method at the 0.2 mm min^{-1} displacement rate.

The membrane filtration performance was assessed using a dead-end filtration unit and the deionized water (DI) flux associated with the experimental membranes measured. The membrane surface area was 0.004 m^2. The water permeability is expressed as the water flux per unit of transmembrane pressure.

$$Pm = \frac{Jv}{TMP} \quad (1)$$

where *Pm* is the water permeability (m^3 m^{-2} h^{-1} MPa^{-1}), *Jv* is the initial water flux (m^3 m^{-2} h^{-1}) and *TMP* is the transmembrane pressure (MPa).

The surface area and pore size distribution of the experimental membranes were characterized using a mercury porosimetry analyzer with the maximum pressure of 206 MPa and the pore diameters of 0.007–322 μm (PoreMaster, Quantachrome Instruments). A *3D laser* scanning confocal *microscope* (Confocal OLS4100 LEXT) with multi-layer mode (black and white image) was employed to examine the distribution of TiO_2 nanoparticles on the ceramic membrane surface. The microstructure of the membrane surface was investigated using a field emission scanning electron microscope (FE-SEM with EDS Hitachi SU5000). The experimental membranes were dried in ambient temperature and underwent the gold sputter coating for 10 s prior to the SEM/EDS analysis.

The functional groups on the membrane surface were analyzed using the Perkin-Elmer spectrum spotlight Fourier transform infrared (FTIR) imaging system. The FTIR spectra analysis was carried out in the middle infrared wavelengths of 4000–600 cm^{-1}.

2.4. Laccase activity

The laccase activities of the laccase- and laccase-TiO_2-membranes were analyzed using the ABTS assay. The enzyme was extracted by stirring the crushed membranes in 10 mL of 0.1 M sodium acetate buffer (pH 5.5) for 30 min. The laccase activity was determined by monitoring the change in the absorbance of the ABTS solution (0.5 mM ABTS in the phosphate-citrate buffer solution) at 420 nm using a spectrophotometer. One unit of laccase activity (U) is defined as the amount of laccase that oxidizes 1 μmol of ABTS per minute.

2.5. Determination of BPA degradation

The BPA removal efficiency of the four experimental membranes was determined using glass vessels each containing 100 mL of 10 mg L^{-1} BPA. The BPA solution was prepared (0.1 g L^{-1} concentration) by dissolving in pure methanol and diluting for the 10 mg L^{-1} solution for further batch-scale experiment. Prior to the BPA removal experiment, the membranes (3.25 × 0.78 cm in diameter and thickness) were washed with Milli-Q water to remove free laccase and then fractured into smaller pieces. The fractured membranes were placed on the stainless steel grate inside the glass vessel, and a magnetic stirrer was used to agitate the BPA solution. To determine the BPA removal performance, the BPA solution samples were taken hourly for an entire period of 8 h. The BPA removal performance is determined by:

$$R(\%) = \left(1 - \frac{C}{C_0}\right) \times 100 \quad (2)$$

where *C* is the remaining concentration (mg L^{-1}) and C_0 is the initial concentration (mg L^{-1}).

The BPA quantification was carried out using gas chromatography mass spectrometry (Shimadzu, GC-MS-QP2010 plus). The BPA solution samples were injected through an RTX-35 MS capillary column with helium as the carrier gas. The BPA concentrations were determined by comparing against the GC/MS library (Wiley7) of standard substances with the detection limit of 1.0 μg L^{-1}.

3. Results and discussion

3.1. The ceramic membrane and the TiO_2-coated membrane

As previously mentioned, the ceramic membranes were fabricated by mixing calcined alumina powders with 1 g L^{-1} CMC solution, where CMC was varied between 0.5, 1.0, 1.5, 2.0 and 2.5 mL per 15 g of calcined alumina powders; and the optimal CMC content, in terms of the bulk density, water absorption and tensile strength of the ceramic membranes, determined. According to Shafiei et al. [16], the binder type and content play an important role in the membrane structure and mechanical strength. Thus, the type and content of the membrane binder should be optimized to enhance the membrane durability. In this research, the alumina ceramic membranes were hydraulically pressed and used as the substrate for the TiO_2 coating and laccase immobilization.

Table 1 tabulates the bulk density, water absorption and tensile strength of the ceramic membranes as a function of the binder (CMC) content. In the table, the bulk density and the tensile strength increased the CMC content increased, which is attributable to the enhanced alumina particle-particle interconnection. However, the CMC content beyond 1.5 mL contributed to a decrease in the bulk density and tensile strength. The excessive binder content increased the post-sintering ceramic membrane porosity, resulting in the lower tensile strength. In addition, the ceramic membranes with 1.5 mL CMC exhibited the lowest water absorption (17.49%), indicating that the ceramic membranes became denser and less porous. In Shafiei et al. [16], variable binder contents in the alumina microfiltration membranes could alter the porosity by 25–49% and also significantly influence their mechanical properties and water permeability. In this

Table 1
Effects of variable binder contents on the ceramic membrane properties

CMC per 15 g calcined alumina powders (mL)	Bulk density (g cm^{-3})	Water absorption (%)	Tensile strength (Mpa)
0.5	2.25	18.07	5.54 ± 0.31
1.0	2.28	17.85	7.13 ± 0.25
1.5	2.29	17.49	7.79 ± 0.39
2.0	2.24	17.67	6.33 ± 0.33
2.5	2.23	17.61	5.77 ± 0.29

Note: The values are the averages of the five membrane samples.

research, the optimal CMC content was 1.5 mL per 15 g alumina powders.

In Nandi et al. [17], the authors fabricated the low-cost microfiltration ceramic membranes with the average pore sizes of 0.55–0.81 μm and the mechanical strength of 3–8 MPa. In addition, Bouzerara et al. [18] developed the ceramic membranes for microfiltration and ultrafiltration with the tensile strengths of 6–15 MPa and variable sintering temperatures. By comparison, in this current research, the porous ceramic membranes, given 1.5 mL CMC per 15 g calcined alumina powders, possessed the tensile strength and the water absorption of 7.79 MPa and 17.49%, respectively.

Figs. 2a–d respectively illustrate the TiO_2-coated ceramic membranes with 0.0, 0.65, 1.3 and 2.6 wt % DispexA40. Under the 0.0 wt % condition, some areas of the membrane surface were absent of TiO_2 and the nanoparticles were not evenly dispersed, due to the agglomeration of TiO_2 nanoparticles (Fig. 2a). With 0.65 wt %, the TiO_2 nanoparticles became more uniformly distributed (Fig. 2b) despite some agglomeration. With 1.3 wt %, the distribution was most uniform (i.e. the optimal dispersant content) (Fig. 2c). With the 2.6 wt % DispexA40, the uneven TiO_2 distribution became noticeable due to the agglomeration induced by the polymeric bridging (Fig. 2d) [19].

Figs. 3a,b respectively illustrate the SEM microstructure and cross-section of the TiO_2-coated ceramic membranes, given the 1.3 wt % dispersant. In Fig. 3a, the SEM image of the TiO_2-membrane shows a smooth surface with uniformly-distributed spherical-shaped TiO_2. In Fig. 3b, the cross-sectional image reveals the TiO_2 composite layer of approximately 5 μm. In addition, the EDS elemental analysis indicated the presence of C, O and Ti, with Ti the dominant element on the membrane surface.

Othman et al. [20] examined the effects of various dispersant contents (polyacrylic acid) on the average cluster size and zeta potential of the TiO_2 suspensions; and documented that the dispersant content that contributed to the monodisperse suspension of the TiO_2 nanoparticles and the highest stability was 3 wt %. Specifically, the use of the dispersant resulted in a higher distribution of Ti elemental coating on the surface vis-à-vis without the dispersant. In this current research, the TiO_2 aqueous suspension containing 1 g L^{-1} of TiO_2 nanoparticles and PEG 1000 (1:1)

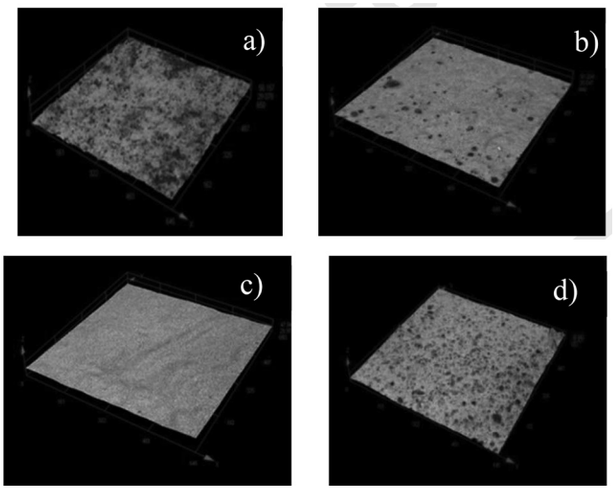

Fig. 2. Confocal microscope images of the surface of the TiO_2-coated ceramic membranes (×20) given DispexA40 of: a) 0%, b) 0.65%, c) 1.3%, d) 2.6 wt %.

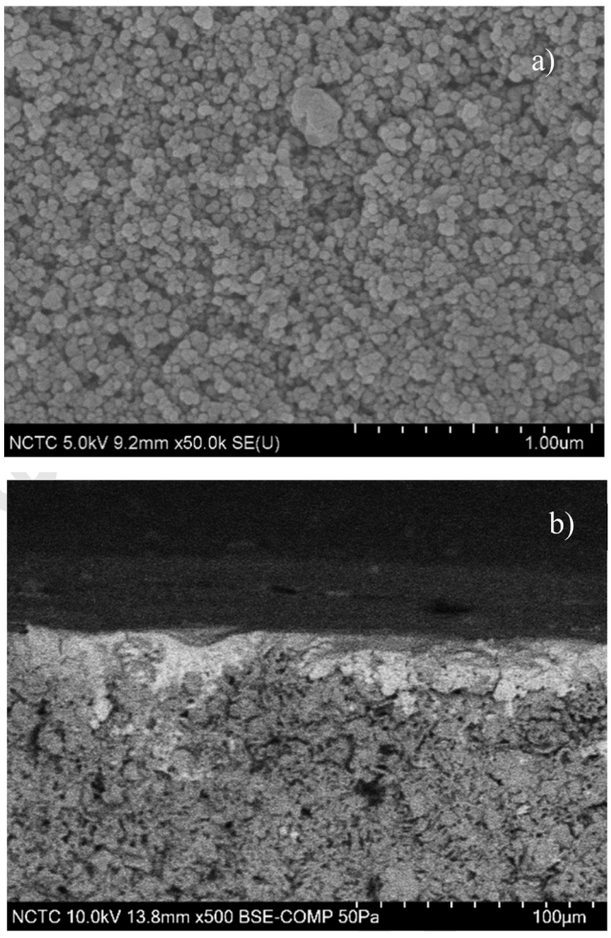

Fig. 3. SEM images of the TiO_2-coated ceramic membranes given 1.3 wt % DispexA40: a) the surface (×50000), b) the cross-section (×500).

and 1.3 wt % DispexA40, was used in the TiO_2 coating of the ceramic membranes.

3.2. The laccase membrane and the laccase-TiO_2-membrane

In this research, the laccase enzyme concentrations were varied between 0, 500, 2500 and 5000 U L^{-1}. The textural properties and membrane surface of the laccase-membrane and the laccase-TiO_2-membrane were characterized using the mercury porosimetry analyzer, SEM, FTIR and pure water permeability test. Table 2 tabulates the pore size, surface area and water permeability of the laccase-membranes and the laccase-TiO_2-membranes, given the various laccase concentrations. Due to the TiO_2 nanoparticles aggregation in the membrane pores, the pore sizes of the laccase-TiO_2-membranes (0.38–0.40 μm) were slightly smaller than those of the laccase-membranes (0.42–0.51 μm). The surface area of the laccase-TiO_2-membranes (1.232–1.947 m^2 g^{-1}) was larger than that of the laccase-membranes (0.822–1.092 m^2 g^{-1}), which is attributable to the mesoporous structure of the TiO_2 coating on the membrane surface. Hou et al. [14] reported that the Brunauer–Emmett–Teller (BET) surface area increased as the TiO_2 loading on the polymeric membrane surface increased. Specifically, fine particulates with high specific area of the TiO_2 nanoparticles formed the mesoporous TiO_2 layer on the membrane surface (Fig. 3a), resulting in an increase in the membrane surface area. TiO_2 also decreased the water permeability, indicating an increase in the mass transfer resistance of the TiO_2 membrane.

Table 2
The pore size, surface area and water permeability of the laccase-membranes and the laccase-TiO_2-membranes given variable laccase concentrations

Support	Laccase conc. (U L^{-1})	Pore size (μm)	Surface Area (m^2 g^{-1})	Water permeability (m^3 m^{-2} h^{-1} MPa^{-1})
Ceramic membrane	0	0.61	0.908	9.15 ± 0.73
	500	0.51	1.092	8.65 ± 0.50
	2500	0.60	0.935	8.91 ± 0.68
	5000	0.42	0.822	8.06 ± 0.47
TiO_2-membrane	0	0.47	2.011	3.77 ± 0.41
	500	0.38	1.947	4.15 ± 0.43
	2500	0.39	1.132	3.40 ± 0.50
	5000	0.40	1.235	3.02 ± 0.38

In fact, the laccase concentrations (500, 2500 and 5000 U L^{-1}) minimally influenced the pore size, surface area and water permeability of the ceramic and TiO_2-coated membranes. The pore sizes of the "pre-immobilized" ceramic membrane (0.61 μm) and TiO_2-membrane (0.47 μm) were considerably larger than the laccase dimensions (7.0 × 5.0 × 5.0 nm^3). The textural properties of the membranes remained porous after the immobilization. Interestingly, Cazes et al. [11] experimented with the gelatin-ceramic membranes immobilized with the laccase enzyme; and reported that the increased gelatin concentration led to the lower water permeability in the membrane with the smaller pore size (0.2 μm) but had no significant effect on the membrane with the larger pore size (1.4 μm).

Fig. 4 illustrates the SEM images of the surface of the laccase-membranes and the laccase-TiO_2-membranes, given the laccase concentrations of 0, 500, 2500 and 5000 U L^{-1}. In Figs. 4a–d (the laccase-membranes), the Al_2O_3 grains exhibited no pinholes or cracks, thus suitable for the microfiltration application. The increased laccase concentration minimally influenced the morphology of the ceramic membrane surface due to the coarseness of Al_2O_3 powders. In Figs. 4e–h, a layer of uniformly distributed TiO_2 was formed on the membrane surface. However, a swelling of the TiO_2 layer occurred with

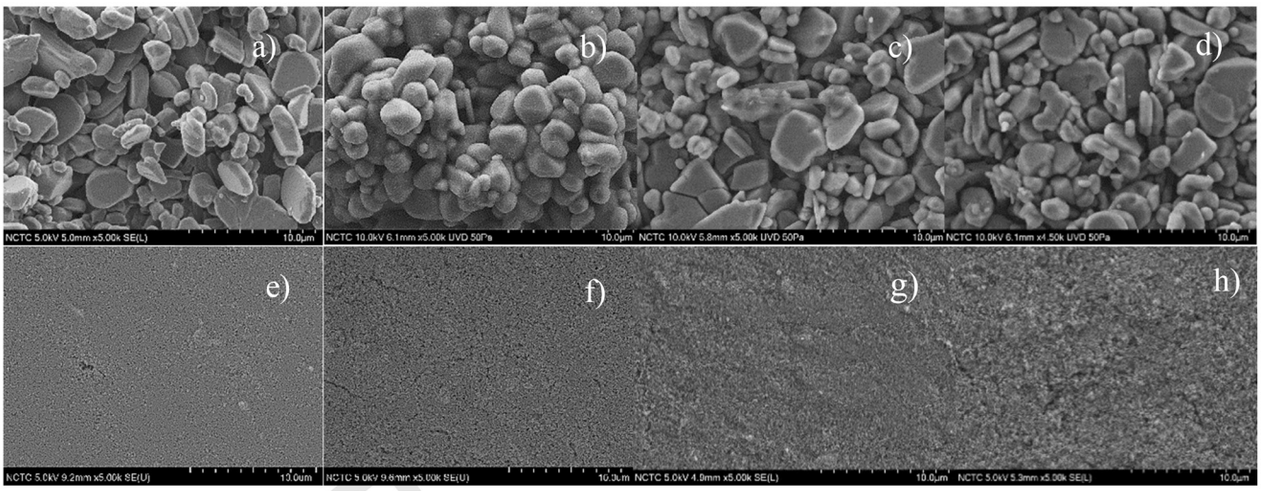

Fig. 4. SEM images of the surface of the laccase-membranes (×5000) with the laccase concentrations of: a) 0, b) 500, c) 2500, d) 5000 U L^{-1}; and those of the surface of the laccase-TiO_2-membranes (×5000) with the laccase concentrations of: e) 0, f) 500, g) 2500, h) 5000 U L^{-1}.

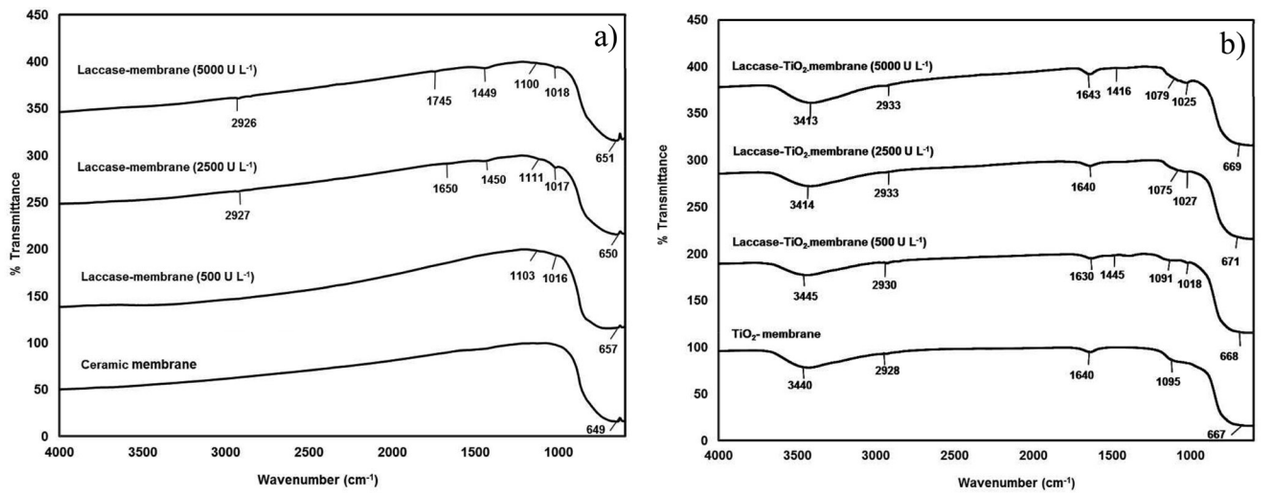

Fig. 5. FTIR spectra of a) the laccase-membranes, b) the laccase-TiO_2-membranes, given the laccase concentrations of 0, 500, 2500 and 5000 U L^{-1}.

5000 U L^{-1} laccase concentration, probably due to the adsorbed laccase accumulating on the coating layer. The accumulation resulted in the enzymatic bridges between TiO_2 nanoparticles and the subsequent swollen surface.

In Fig. 5a, the FTIR spectra of the non-enzymatic and laccase-immobilized ceramic membranes were somewhat similar. The non-enzymatic ceramic membrane exhibited the absorption peak at 649 cm^{-1}, which is the characteristic absorption band of α-Al_2O_3 with a corundum structure [21]. The absorption bands of the laccase-membranes were relatively similar to that of the non-enzymatic membrane, except for other weak peaks, e.g., 2926 (CH), 1650 (CONH) and 1100–1018 cm^{-1} (CO), which were related to the characteristic chemical groups of proteins [22]. The weak protein peaks were attributable to the low chemical interaction between the laccase enzyme and the Al_2O_3 ceramic membrane, suggesting that the laccase immobilization was probably the result of membrane adsorption.

In Fig. 5b, due to the Ti-O stretching vibration of the TiO_2 layer on the membrane surface, the absorption peaks associated with the laccase-TiO_2-membranes of the various laccase concentrations (i.e., 0, 500, 2500, 5000 U L^{-1}) lay between 667–669 cm^{-1}. Furthermore, the absorption bands were observed at 3440 cm^{-1} and 1640 cm^{-1}, attributable to the O–H stretching vibration peak of the hydroxyl group and the bending vibration of the surface H–OH [23].

The absorption bands associated with the protein chemical groups (CH, CONH and CO) of the laccase-TiO_2-membranes (Fig. 5b) were more intense than the laccase membranes (Fig. 5a), indicating the enhanced binding interaction between the enzyme and the TiO_2-coated ceramic membranes. The O–H group on the laccase-TiO_2-membrane surface, as shown in Fig. 5b, could functionalize with the enzyme via covalent bonding, resulting in the stronger chemical interactions. According to Hou et al. [14], the covalent bonding formed between the laccase and TiO_2 on the TiO_2-coated PVDF membranes enhanced the laccase attachment and the subsequent higher laccase loading, whereas the low laccase loading of the non-TiO_2 PVDF membranes was largely due to the weak van der Waals force between the laccase and the membrane surface.

Fig. 6 illustrates the laccase activity of the laccase-membranes and the laccase-TiO_2-membranes, given the enzyme concentrations of 500, 2500 and 5000 U L^{-1}. The laccase concentration and its activity were positively correlated for both membranes. The maximum laccase activity for the laccase-membranes and the laccase-TiO_2-membranes, given 5000 U L^{-1} laccase concentration, were 0.29 ± 0.01 U cm^{-2} and 0.38 ± 0.02 U cm^{-2}, respectively. By comparison, given 5000 U L^{-1} laccase concentration, the higher laccase activity of 0.41 ± 0.04 U cm^{-2} was achieved with the 0.45 μm PVDF membranes with three TiO_2 coating cycles, compared with that of 0.131 ± 0.013 U cm^{-2} with

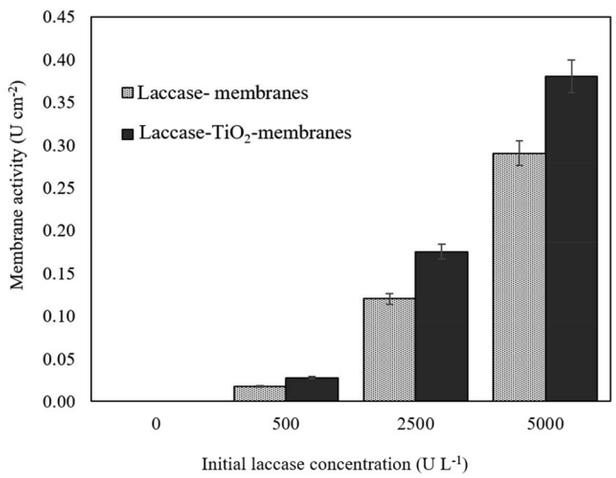

Fig. 6. Effects of various laccase concentrations on the membrane activity of the laccase- and laccase-TiO_2-membranes.

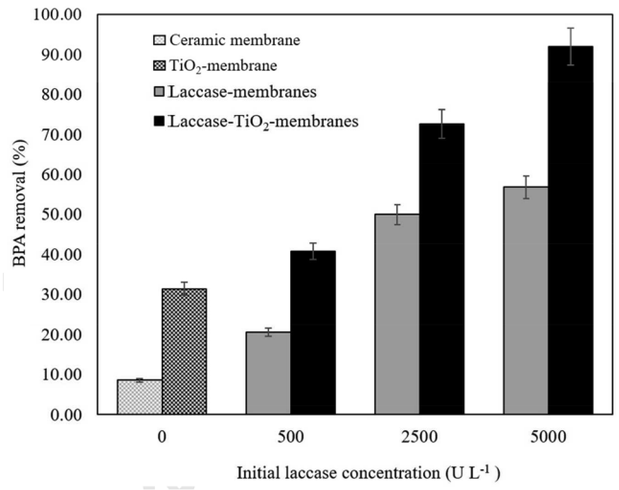

Fig. 7. Comparison of the BPA removal efficiency of the ceramic membrane, the TiO_2-membrane, the laccase-membranes and the laccase-TiO_2-membranes under visible light.

the TiO_2 nanoparticles blended in the *polyethersulfone* (PES) membranes [14]. In fact, the laccase activity of this current research is comparable to Hou et al. [14], indicating the effectiveness of the laccase immobilization on the ceramic membranes and the TiO_2-coated membranes.

In fact, the higher laccase activity of the laccase-TiO_2-membranes vis-a-vis the laccase-membranes could be attributed to: (i) the larger surface area of the TiO_2-coated membrane (Table 2) which provides more anchor points for the interaction between the laccase and the ceramic membrane; (ii) the smaller membrane pore sizes of the mesoporous structure of the TiO_2 layer (Table 2 and Fig. 4), which enhance the physical and chemical interactions of the laccase immobilization; and (iii) the elevated chemical interaction through covalent binding between the membrane surface and the enzyme (Fig. 5b).

3.3. The BPA removal performance

The BPA removal performance of the ceramic membrane, the TiO_2-membrane, the laccase-membrane and the laccase-TiO_2-membrane under visible light was investigated, and the results are compared in Fig. 7. Without the laccase immobilization (0 U L^{-1}), the BPA removal efficiency of the ceramic membrane was only 9%, indicating a low affinity between the ceramic membrane (hydrophilic in nature) and BPA (moderately hydrophobic). The BPA removal efficiency increased to 31% with the non-enzymatic TiO_2-membrane. According to Dong et al. [24], the carbon-doped TiO_2 improved the degradation of organic pollutants through the higher photocatalytic performance (under visible light) and the enhanced organic-pollutants adsorption capacity of the membranes.

In this research, the enhanced BPA removal of the TiO_2-membranes could possibly be attributed to the modification effects of the carbon compounds in PEG 1000 and DispexA40. The carbon in PEG 1000 and DispexA40 could possibly be doped in the TiO_2 matrix and thus improved the visible light absorption of TiO_2, leading to an increase in the BPA removal performance. In addition, the EDS elemental analysis identified approximately 3.5% carbon on the surface of the TiO_2-membranes, indicating that the heavy fraction of the carbon compound remained in the TiO_2 coating even after the binder/dispersant removal at 540°C. The residual carbon from the incomplete removal of the binder or dispersant in the calcination step could narrow the TiO_2 band gap energy, resulting in the enhanced visible light absorption of the TiO_2-membranes [25].

With the laccase immobilization, the BPA concentrations decelerated during the first four hours and then declined at a slow pace for the remaining period (Figs. 8a,b). The BPA removal efficiencies of the laccase-membranes and the laccase-TiO_2-membranes were positively correlated with the laccase concentration, with the stronger correlation for the laccase-TiO_2-membranes. The BPA removal efficiencies of the 500, 2500 and 5000 U L^{-1} laccase-membranes were 20, 50 and 57%, respectively, and 41, 73, and 93% for the corresponding

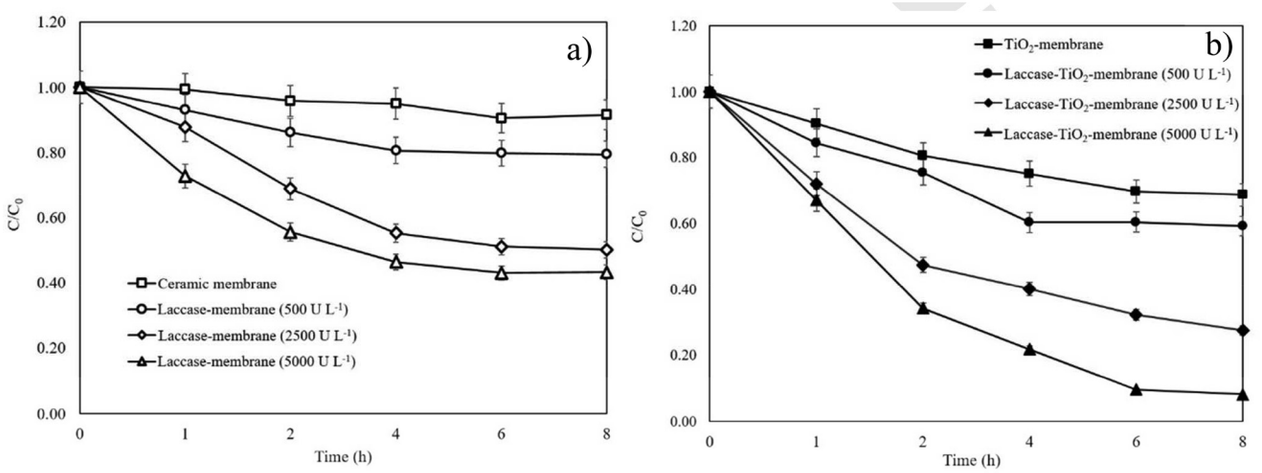

Fig. 8. BPA degradation relative to time under variable laccase concentrations: (a) the ceramic and laccase-membranes, (b) the TiO_2 and laccase-TiO_2-membranes.

laccase-TiO_2-membranes. The findings indicated that TiO_2 enhanced the BPA removal performance because, in addition to its higher photocatalytic activity under visible light, TiO_2 increased the membrane surface area, formed the mesoporous structure and induced the stronger binding between laccase and the membrane surface.

4. Conclusions

This research has investigated the effects of TiO_2 on the laccase enzyme immobilization, given the laccase concentrations of 0, 500, 2500 and 5000 U L^{-1}, and the BPA removal performance of four types of the ceramic membranes: the ceramic membranes, the TiO_2-membranes, the laccase-membranes and the laccase-TiO_2-membranes. The results indicated that TiO_2 enhanced the laccase immobilization as a result of the increased membrane surface area, the mesoporous structure and the stronger laccase-membrane binding. In addition, the highest BPA removal efficiency of 93% was achieved with the 5000 U L^{-1} laccase-TiO_2-membrane. Moreover, by comparison, the BPA removal efficiency of the TiO_2-membrane (31%) was higher than that of the ceramic membrane (9%) and the 500 U L^{-1} laccase-membrane (20%). The more efficient BPA removal was attributable to the improved degradation of organic pollutants as a result of higher photocatalytic performance under visible light and the enhanced organic-pollutants adsorption capacity of the TiO_2-coated membrane.

Acknowledgments

The authors would like to extend deep gratitude to the Kurita Water and Environmental Foundation (KWEF, 2015) for the research funding. Sincere appreciation also goes to the National Metal and Materials Technology Center (MTEC), National Science and Technology Development Agency (NSTDA) for the facility and instrumentation support.

References

[1] L.N. Vandenberg, R. Hauser, M. Marcus, N. Olea, W.V. Welshons, Human exposure to bisphenol A (BPA), Reprod. Toxicol., 24 (2007) 139–177.
[2] P. Kjeldsen, M.A. Barlaz, A.P. Rooker, A. Baun, A. Ledin, T. H. Christensen, Present and long-term composition of MSW landfill leachate: a review. Crit. Rev. Environ. Sci. Technol., 32 (2002) 297–336.
[3] Y.Q. Huang, C.K.C. Wong, J.S. Zheng, H. Bouwman, R. Barra, B. Wahlström, L. Neretin, M.H. Wong, Bisphenol A (BPA) in China: a review of sources, environmental levels, and potential human health impacts, Environ. Int., 42 (2012) 91–99.
[4] N. Bolong, A.F. Ismail, M.R. Salim, T. Matsuura, A review of the effects of emerging contaminants in wastewater and options for their removal, Desalination, 239 (2009) 229–246.
[5] J.M. Santos, D.A. Putt, M. Jurban, A. Joiakim, K. Friedrich, H. Kim, Differential BPA levels in sewage wastewater effluents from metro Detroit communities, Environ. Monit. Assess., 188 (2016) 585.
[6] Y. Luo, W. Guo, H.H. Ngo, L.D. Nghiem, F.I. Hai, J. Zhang, S. Liang, X.C.A. Wang, Review on the occurrence of micropollutants in the aquatic environment and their fate and removal during wastewater treatment, Sci. Total Environ., 473 (2014) 619–641.
[7] H. Cabana, J.P. Jones, S.N. Agathos, Elimination of endocrine disrupting chemicals using white rot fungi and their lignin modifying enzymes: a review, Eng. Life Sci., 7 (2007) 429–456.
[8] H. Cabana, J.P. Jones, S.N. Agathos, Preparation and characterization of cross-linked laccase aggregates and their application to the elimination of endocrine disrupting chemicals, J. Biotechnol., 132 (2007) 23–31.
[9] M. Fernández-Fernández, M.Á. Sanromán, D. Moldes, Recent developments and applications of immobilized laccase, Biotechnol. Adv., 31 (2013) 1808–1825.
[10] V. Chea, D. Paolucci-Jeanjean, M.P. Belleville, J. Sanchez, Optimization and characterization of an enzymatic membrane for the degradation of phenolic compounds, Catal. Today., 193 (2012) 49–56.
[11] M.D. de Cazes, M.P. Belleville, M. Mougel, H. Kellner, J. Sanchez-Marcano, Characterization of laccase-grafted ceramic membranes for pharmaceuticals degradation, J. Membr. Sci., 476 (2015) 384–393.
[12] R.J. Ciora, P.K. Liu, Ceramic membranes for environmental related applications, Fluid/Part. Sep. J., 15 (2003) 51–60.
[13] K.K.O. Silva, C.A. Paskocimas, F.R. Oliveira, J.H. Nascimento, A. Zille, Development of porous alumina membranes for treatment of textile effluent, Desal. Water. Treat., 57 (2016) 2640–2648.
[14] J. Hou, G. Dong, Y. Ye, V. Chen, Enzymatic degradation of bisphenol-A with immobilized laccase on TiO_2 sol–gel coated PVDF membrane, J. Membr. Sci. 469 (2014) 19–30.
[15] J. Hou, G. Dong, Y. Ye, V. Chen, Laccase immobilization on titania nanoparticles and titania-functionalized membranes, J. Membr. Sci., 452 (2014) 229–240.
[16] K. Shafiei, M. Kazemimoghaddam, T. Mohammadi, S. Ghanbari Pakdehi, An investigation on manufacturing of alumina microfiltration membranes, Desalin. Water. Treat., 53 (2015) 2429–2436.
[17] B.K. Nandi, R. Uppaluri, M.K. Purkait, Preparation and characterization of low cost ceramic membranes for micro-filtration applications, Appl. Clay Sci., 42 (2008) 102–110.
[18] F. Bouzerara, A. Harabi, S. Achour, A. Larbot, Porous ceramic supports for membranes prepared from kaolin and dolomite mixtures, J. Eur. Ceram. Soc., 26 (2006) 1663–1671.
[19] N. Veronovski, P. Andreozzi, C. La Mesa, M. Sfiligoj-Smole, Stable TiO_2 dispersions for nanocoating preparation, Surf. Coat. Tech., 204 (2010) 1445–1451.
[20] S.H. Othman, S.A. Rashid, T.I.M. Ghazi, N. Abdullah, Dispersion and stabilization of photocatalytic TiO_2-nanoparticles in aqueous suspension for coatings applications, J. Nanomater., 2012 (2012) 1–10.
[21] J. Li, Y. Pan, C. Xiang, Q. Ge, J. Guo, Low temperature synthesis of ultrafine α-Al_2O_3 powder by a simple aqueous sol–gel process, Ceram. Int., 32 (2006) 587–591.
[22] K. Mohajershojaei, N.M. Mahmoodi, A. Khosravi, Immobilization of laccase enzyme onto titania nanoparticle and decolorization of dyes from single and binary systems, Biotechnol. Bioprocess Eng., 20 (2015) 109–116.
[23] S. Buddee, S. Wongnawa, P. Sriprang, C. Sriwong, Curcumin-sensitized TiO_2 for enhanced photodegradation of dyes under visible light, J. Nanopart. Res., 16 (2014) 2336.
[24] H. Dong, G. Zeng, L. Tang, C. Fan, C. Zhang, X. He, Y. He, An overview on limitations of TiO2-based particles for photocatalytic degradation of organic pollutants and the corresponding countermeasures, Water. Res., 79 (2015) 128–146.
[25] S. Sakthivel, H. Kisch, Daylight photocatalysis by carbon modified titanium dioxide, Angew. Chem. Int. Ed., 42 (2003) 4908–4911.